Korean J. Chem. Eng., **27**(3), 955-961 (2010)
DOI: 10.1007/s11814-010-0151-5

Frequency response analysis of the constant molar flow semi-batch adsorption vessel containing core-shell composites

In-Soo Park†

Department of Fire and Disaster Prevention Engineering, Kyungnam University, Masan 631-701, Korea
(*Received 24 August 2009 • accepted 28 October 2009*)

Abstract−Frequency response behavior of the constant molar flow semi-batch adsorption vessel containing core-shell composites is theoretically investigated. The periodic modulation of the inlet molar flow-rate into the vessel is considered as the forcing function to the response. Under the interaction between the core-phase and the shell-phase of the composite, both the response of the core-phase and the response of the shell-phase subject to the forcing function exhibit their own peaks on the out-of-phase characteristic curve and their own plateaus on the in-phase characteristic curve, respectively. The model to be developed will include the local linear equilibriums at the fluid-particle interface and at the intraparticle core-shell interface, the external diffusion, the intraparticle diffusion in the outer shell-phase, and the intraparticle diffusion in the inner core-phase.

Key words: Frequency Response, Core-shell Composite, Adsorption Vessel, Transfer Function, Characteristic Function

INTRODUCTION

In the frequency response (FR) technique for the study of the adsorption equilibrium and dynamics, the system is perturbed about an equilibrium state by periodic variation of some system variables, and then the responses of the system variables forced by the variation are investigated to characterize the system. As the forcing function to FR, a periodic modulation of the reservoir volume of a batch system was originally considered [1-7]. More recently, a periodic modulation of inlet flow concentration [8] and a periodic modulation of inlet molar flow-rate [9-12] of a flow system were considered as the forcing function. With the modulation of inlet molar flow-rate in a flow system, large perturbation of forcing function can be allowed for better measurements of system variables under the linear limitation of the FR technique. Since the in-phase (IP) and the out-of-phase (OP) characteristic functions of FR for the modulation of inlet molar flow-rate have the same functional dependence of system variables as those for modulation of the reservoir volume [9,10], the theoretical analyses of FRs subject to the two different types of forcing functions are practically the same.

Composite particles with core-shell structure may be useful in many applications, such as development of adsorbents, catalysts, calorimetric sensors, optoelectronic devices, and bioprocessing devices [13-18]. When the inner core is impermeable, the composite is called an inert-core adsorbent, since this composite was reported to be suitable as an adsorbent for stable expansion at high flow rates in expanded-bed. When the inner core is permeable, the composite is called a core-shell composite as it is. In previous works [19-21] we presented exact analytical solutions for the step and the frequency responses of a constant molar flow semi-batch adsorption vessel containing particles with core-shell structure.

An outstanding advantage of the FR technique is its ability to discriminate between various mass transfer mechanisms by examining the response over a large frequency spectrum [5,22]. In addition, the FR technique allows for the determination of system characteristics (such as the amplitude and the phase angle of FR) over much smaller changes in the system conditions than are typically used for the step response technique.

The aim of this work is to extend the step response analysis of the previous work [21] for the constant molar flow semi-batch adsorption vessel containing permeable core-shell composites to investigate FR characteristics of the system subject to a periodic modulation of inlet molar flow-rate. The model to be developed will include both the equilibrium interferences (at the fluid-particle interface and at the intraparticle core-shell interface) and the diffusion interferences (in the external film, in the outer shell-phase and in the inner core-phase). Responses for cases of impermeable core-shell composites (i.e., inert-core adsorbents) and homogeneous particles can be obtained by taking appropriate limits.

SYSTEM DESCRIPTION

1. Mass Balance

With linear adsorption equilibriums at the outer surface of the composite and at the intraparticle core-shell interface, modeling of the constant molar flow semi-batch adsorption vessel containing permeable core-shell composites gives rise to the following mass balance equations in dimensionless form, with dimensionless variables and parameters defined in Table 1 [21]:

Mass Balance in Inner Permeable Core-Phase:

$$\frac{\partial A_1}{\partial \tau} = a^2\left(\frac{\partial^2 A_1}{\partial x^2} + \frac{2}{x}\frac{\partial A_1}{\partial x}\right) \qquad (0 \le x \le x_C) \tag{1a}$$

$$\text{at } \tau = 0 \qquad A_1 = 0 \tag{1b}$$

$$\text{at } x = 0 \qquad \frac{\partial A_1}{\partial x} = 0 \tag{1c}$$

†To whom correspondence should be addressed.
E-mail: ispark@kyungnam.ac.kr

Table 1. Definition of dimensionless variables and parameters

$$A_b=\frac{C_b}{C_0};\quad A=\frac{C}{K_2C_0};\quad A_1=\frac{C_1}{K_2C_0};\quad A_2=\frac{C_2}{K_2C_0};\quad a=\sqrt{D_1/D_2};$$
$$x=\frac{r}{R};\quad x_C=\frac{R_C}{R};\quad \beta_0=\frac{K_2V}{V_b};\quad \xi=\frac{k_fR}{K_2D_2};\quad \tau=\frac{D_2t}{R^2};$$
$$\Omega=\frac{R^2/D_2}{V_bC_0/\dot{N}};\quad \omega^*=\omega\left(\frac{R^2}{D_2}\right)$$

Mass Balance in Outer Shell-Phase:

$$\frac{\partial A_2}{\partial\tau}=\frac{\partial^2A_2}{\partial x^2}+\frac{2}{x}\frac{\partial A_2}{\partial x}\qquad (x_C\le x\le 1) \tag{2a}$$

at $\tau=0$ $\quad A_2=0$ (2b)

Mass Balance around Adsorption Vessel:

$$\frac{dA_b}{d\tau}+\beta_0\frac{d\langle A\rangle}{d\tau}=\Omega X(\tau);\quad \langle A\rangle=(1-x_C^3)\langle A_2\rangle+x_C^3\langle A_1\rangle \tag{3a}$$

at $\tau=0$ $\quad A_b=0$ (3b)

where

$$\langle A_2\rangle=\frac{3}{1-x_C^3}\int_{x_C}^{1}x^2A_2dx;\qquad \langle A_1\rangle=\frac{3}{x_C^3}\int_0^{x_C}x^2A_1dx \tag{3c}$$

Three Boundary Conditions and Two Linear Equilibrium Relationships:

$$\left.\frac{\partial A_1}{\partial x}\right|_{x=0}=0 \tag{4a}$$

$$\left[\frac{\partial A_2}{\partial x}\right]_{x=1}=\xi(A_b-A_b|_{x=1}) \tag{4b}$$

$$a^2\left.\frac{\partial A_1}{\partial x}\right|_{x=x_C}=\left.\frac{\partial A_2}{\partial x}\right|_{x=x_C} \tag{4c}$$

$$A_2|_{x=1}=A_b|_{x=1} \tag{4d}$$

$$A_1|_{x=x_C}=K_1A_2|_{x=x_C} \tag{4e}$$

For FR of the semi-batch adsorption vessel with periodical modulation of inlet molar flow-rate, the forcing function is:

$$X(\tau)=(1+\nu\sin(\omega^*\tau))U(\tau) \tag{5}$$

where $U(\tau)$ is the unit step function.

2. Solution in Laplace Domain

From Eq. (3), the overall transfer function G(s) which relates the forcing function to the response in Laplace domain is given by

$$G(s)\equiv\frac{\overline{A}_b}{\Omega\overline{X}}=\frac{1}{s(1+\beta_0F(s))} \tag{6}$$

in terms of the vessel transfer function F(s).

The vessel transfer function is given as follows [21]:

$$F(s)=F_1(s)+F_2(s); \tag{7a}$$

$$F_1(s)\equiv\frac{\langle\overline{A}_1\rangle}{\overline{A}_b}=\frac{f_{21}(s)}{f_1(s)};\qquad F_2(s)\equiv\frac{\langle\overline{A}_2\rangle}{\overline{A}_b}=\frac{f_{22}(s)}{f_1(s)}; \tag{7b}$$

$$f_1(s)=\left[\left(1-\frac{1}{\xi}\right)\sinh(\sqrt{s})+\frac{\sqrt{s}}{\xi}\cosh(\sqrt{s})\right]-\left[\left(1-\frac{1}{\xi}\right)\cosh(\sqrt{s})+\frac{\sqrt{s}}{\xi}\sinh(\sqrt{s})\right]Q(s) \tag{7c}$$

$$f_{21}(s)=\frac{3}{s}(a^2K_1)\left[\frac{x_C\sqrt{s}}{a}\coth\left(\frac{x_C\sqrt{s}}{a}\right)-1\right][\sinh(x_C\sqrt{s})-Q(s)\cosh(x_C\sqrt{s})] \tag{7d}$$

$$f_{22}(s)=\frac{3}{s}\left\{\begin{bmatrix}(\sqrt{s}\cosh(\sqrt{s})-\sinh(\sqrt{s}))\\-(x_C\sqrt{s}\cosh(x_C\sqrt{s})-\sinh(x_C\sqrt{s}))\end{bmatrix}+\begin{bmatrix}(\cosh(\sqrt{s})-\sqrt{s}\sinh(\sqrt{s}))\\-(\cosh(x_C\sqrt{s})-x_C\sqrt{s}\sinh(x_C\sqrt{s}))\end{bmatrix}Q(s)\right\} \tag{7e}$$

$$Q(s)=\frac{q(s)\sinh(x_C\sqrt{s})-[\sinh(x_C\sqrt{s})-x_C\sqrt{s}\cosh(x_C\sqrt{s})]}{q(s)\cosh(x_C\sqrt{s})-[\cosh(x_C\sqrt{s})-x_C\sqrt{s}\sinh(x_C\sqrt{s})]} \tag{7f}$$

$$q(s)=a^2K_1\left[1-\frac{x_C\sqrt{s}}{a}\coth\left(\frac{x_C\sqrt{s}}{a}\right)\right] \tag{7g}$$

Applying Laplace transform to Eq. (5), we have

$$\overline{X}=\frac{1}{s}+\nu\left(\frac{\omega^*}{s^2+(\omega^*)^2}\right) \tag{8}$$

Substituting Eq. (8) into Eq. (6), we obtain the solution for the sinusoidal response in Laplace domain:

$$\frac{\overline{A}_b}{\Omega}=\frac{1}{s(1+\beta_0F(s))}\left[\frac{1}{s}+\nu\left(\frac{\omega^*}{s^2+(\omega^*)^2}\right)\right] \tag{9}$$

FREQUENCY RESPONSE

1. Characteristic Function of Frequency Response

We define the IP characteristic function and OP characteristic function of FR as the real part and the negative of the imaginary part of vessel transfer function when $s\to i\omega^*$, respectively:

$$F_R\equiv\mathrm{Re}\{\lim_{s\to i\omega^*}[F(s)]\};\quad F_I\equiv\mathrm{Im}\{\lim_{s\to i\omega^*}[F(s)]\} \tag{10}$$

where

$$F_R=R_{1R}+F_{2R};\qquad F_I=F_{1I}+F_{2I} \tag{11a}$$

$$F_{1R}=\frac{f_{1R}f_{21R}+f_{1I}f_{21I}}{f_{1R}^2+f_{1I}^2};\qquad F_{1I}=\frac{f_{1R}f_{21I}-f_{1I}f_{21R}}{f_{1R}^2+f_{1I}^2} \tag{11b}$$

$$F_{2R}=\frac{f_{1R}f_{22R}+f_{1I}f_{22I}}{f_{1R}^2+f_{1I}^2};\qquad F_{2I}=\frac{f_{1R}f_{22I}-f_{1I}f_{22R}}{f_{1R}^2+f_{1I}^2} \tag{11c}$$

$$f_{1R}\equiv\mathrm{Re}\{\lim_{s\to i\omega^*}[f_1(s)]\};\qquad f_{1I}\equiv-\mathrm{Im}\{\lim_{s\to i\omega^*}[f_1(s)]\} \tag{11d}$$

$$f_{21R}\equiv\mathrm{Re}\{\lim_{s\to i\omega^*}[f_{21}(s)]\};\qquad f_{21I}\equiv-\mathrm{Im}\{\lim_{s\to i\omega^*}[f_{21}(s)]\} \tag{11e}$$

$$f_{22R}\equiv\mathrm{Re}\{\lim_{s\to i\omega^*}[f_{22}(s)]\};\qquad f_{22I}\equiv-\mathrm{Im}\{\lim_{s\to i\omega^*}[f_{22}(s)]\} \tag{11f}$$

Characteristic functions in Eq. (11) can be obtained by the substitution of $s=i\omega^*$ into Eq. (7):

$$f_{1R}=\left\{\left[\frac{u}{\xi}-\left(1-\frac{1}{\xi}\right)Q_R\right]\cos u+(Q_R-Q_I)\frac{u}{\xi}\sin u\right\}\cosh u+\left\{\left[\left(1-\frac{1}{\xi}\right)-(Q_R+Q_I)\frac{u}{\xi}\right]\cos u-\left[\frac{u}{\xi}+\left(1-\frac{1}{\xi}\right)Q_I\right]\sin u\right\}\sinh u \tag{12a}$$

$$f_{1I}=\left\{-\left[\frac{u}{\xi}+\left(1-\frac{1}{\xi}\right)Q_I\right]\cos u-\left[\left(1-\frac{1}{\xi}\right)-(Q_R+Q_I)\frac{u}{\xi}\right]\sin u\right\}\cosh u+\left\{(Q_R-Q_I)\frac{u}{\xi}\cos u+\left[\left(1-\frac{1}{\xi}\right)Q_R-\frac{u}{\xi}\right]\sin u\right\}\sinh u \tag{12b}$$

$$f_{22R}=\frac{3}{2u^2}\left\{\begin{array}{l}[(u-Q_I)\cos u-(1+(Q_R+Q_I)u)\sin u]\cosh u\\ -[(Q_R-Q_I)u\cos u-(u+Q_R)\sin u]\sinh u\\ +[(Q_I-x_C u)\cos x_C u\\ +(1+(Q_R+Q_I)x_C u)\sin x_C u]\cosh x_C u\\ +[(Q_R-Q_I)x_C u\cos x_C u\\ -(Q_R+x_C u)\sin x_C u]\sinh x_C u\end{array}\right\} \tag{12c}$$

$$f_{22I}=\frac{3}{2u^2}\left\{\begin{array}{l}[(Q_R+u)\cos u+(Q_R-Q_I)u\sin u]\cosh u\\ -[(1+(Q_R+Q_I)u)\cos u-(Q_I-u)\sin u]\sinh u\\ -[(Q_R+x_C u)\cos x_C u\\ +(Q_R-Q_I)x_C u\sin x_C u]\cosh x_C u\\ +[(1+(Q_R+Q_I)x_C u)\cos x_C u\\ -(Q_I-x_C u)\sin x_C u]\sinh x_C u\end{array}\right\} \tag{12d}$$

$$f_{21R}=\frac{3}{2u^2}\left\{\begin{array}{l}[(q_R Q_I-q_I Q_R)\cos x_C u-q_R\sin x_C u]\cosh x_C u\\ +[q_I\cos x_C u+(q_R Q_R+q_I Q_I)\sin x_C u]\sinh x_C u\end{array}\right\} \tag{12e}$$

$$f_{21I}=\frac{3}{2u^2}\left\{\begin{array}{l}[(q_R Q_R+q_I Q_I)\cos x_C u-q_I\sin x_C u]\cosh x_C u\\ -[q_R\cos x_C u+(q_R Q_I-q_I Q_R)\sin x_C u]\sinh x_C u\end{array}\right\} \tag{12f}$$

$$Q_R\equiv \mathrm{Re}\{\lim_{s\to i\omega^*}[Q(s)]\}$$
$$=\frac{\begin{array}{l}2x_C u[(q_R-1)-q_I]\cosh(2x_C u)\\ +[(q_R-1)^2+q_I^2+2x_C^2u^2]\sinh(2x_C u)\end{array}}{\left\{\begin{array}{l}[(q_R-1)^2+q_I^2-2x_C^2u^2]\cos(2x_C u)\\ -2x_C u[(q_R-1)+q_I]\sin(2x_C u)\\ +[(q_R-1)^2+q_I^2+2x_C^2u^2]\cosh(2x_C u)\\ +2x_C u[(q_R-1)-q_I]\sinh(2x_C u)\end{array}\right\}} \tag{12g}$$

$$Q_I\equiv -\mathrm{Im}\{\lim_{s\to i\omega^*}[Q(s)]\}$$
$$=\frac{\begin{array}{l}-2x_C u[(q_R-1)+q_I]\cos(2x_C u)\\ -[(q_R-1)^2+q_I^2-2x_C^2u^2]\sin(2x_C u)\end{array}}{\left\{\begin{array}{l}[(q_R-1)^2+q_I^2-2x_C^2u^2]\cos(2x_C u)\\ -2x_C u[(q_R-1)+q_I]\sin(2x_C u)\\ +[(q_R-1)^2+q_I^2+2x_C^2u^2]\cosh(2x_C u)\\ +2x_C u[(q_R-1)-q_I]\sinh(2x_C u)\end{array}\right\}} \tag{12h}$$

$$q_R\equiv \mathrm{Re}\{\lim_{s\to i\omega^*}[q(s)]\}$$
$$=a^2K_1\left[1+\left(\frac{x_C u}{a}\right)\frac{\sin(2x_C u/a)+\sinh(2x_C u/a)}{\cos(2x_C u/a)-\cosh(2x_C u/a)}\right] \tag{12i}$$

$$q_I\equiv -\mathrm{Im}\{\lim_{s\to i\omega^*}[q(s)]\}$$
$$=a^2K_1\left[\left(\frac{x_C u}{a}\right)\frac{\sin(2x_C u/a)-\sinh(2x_C u/a)}{\cos(2x_C u/a)-\cosh(2x_C u/a)}\right] \tag{12j}$$

$$u=\sqrt{\omega^*/2} \tag{12k}$$

2. Frequency Response

Rearranging Eq. (9), we have:

$$\frac{\overline{A}_b}{\Omega}=\left(\frac{\overline{A}_b}{\Omega}\right)_{step}+\left(\frac{\overline{A}_b}{\Omega}\right)_{sine} \tag{13a}$$

$$\left(\frac{\overline{A}_b}{\Omega}\right)_{step}=\frac{1}{s^2[1+\beta_0 F(s)]} \tag{13b}$$

$$\left(\frac{\overline{A}_b}{\Omega}\right)_{sine}=(\nu\omega^*)\frac{1}{s(s^2+(\omega^*)^2)[1+\beta_0 F(s)]} \tag{13c}$$

Taking the inverse transform of Eq. (13) by using the method of residues, we can obtain the sinusoidal response in the time domain. Then FR can be obtained by taking the limit when $\tau\to\infty$ as described below.

First, the step part of FR can be obtained by taking the inverse transform of Eq. (13b), which is given in the reference [21]; then we obtain the ultimate response by taking the limit when $\tau\to\infty$:

$$\left(\frac{A_b}{\Omega}\right)_{step,\infty}=\delta_0\tau+\beta_0[1+(K_1-1)x_C^3]\delta_0^2(\delta_f+\delta_a) \tag{14a}$$

$$\delta_0=\frac{1}{1+\beta_0[1+(K_1-1)x_C^3]} \tag{14b}$$

$$\delta_f=\frac{1}{3\xi}[1+(K_1-1)x_C^3] \tag{14c}$$

$$\delta_a=\frac{1}{15}\left[1+\frac{4(K_1-1)(x_C^3-x_C^5)+5(K_1-1)^2(x_C^5-x_C^6)+\left(\frac{1-a^2}{a^2}\right)K_1x_C^5}{1+(K_1-1)x_C^3}\right] \tag{14d}$$

Second, the sinusoidal part of FR can be also obtained by taking the inverse transform of Eq. (13c) by using the method of residues; then we obtain the ultimate response by taking the limit when $\tau\to\infty$:

$$\left(\frac{A_b}{\Omega}\right)_{sine,\infty}=\frac{\nu}{\omega^*[1+\beta_0(1+(K_1-1)x_C^3)]}+\nu AR\sin(\omega^*\tau+PS) \tag{15a}$$

$$AR=\frac{1}{\omega^*\sqrt{(\beta_0F_I)^2+(1+\beta_0F_R)^2}} \tag{15b}$$

$$PS=\phi-\frac{\pi}{2};\quad \phi=\tan^{-1}\left(\frac{\beta_0F_I}{1+\beta_0F_R}\right) \tag{15c}$$

where the first term on the RHS of Eq. (15a) is the residue for the single pole at s=0, and the second term on the RHS of Eq. (15a) is the residue for the conjugate complex pole at $s^2+(\omega^*)^2=0$, respectively. AR and PS are the amplitude-ratio and the phase-shift characteristic functions of FR, respectively. Note that the sum of residues for the infinite number of poles at $(1+\beta_0F(s)=0)$ is dissipated when $\tau\to\infty$.

Finally, FR is given by:

$$\frac{A_b}{\Omega}=\left(\frac{A_b}{\Omega}\right)_{step,\infty}+\left(\frac{A_b}{\Omega}\right)_{sine,\infty} \tag{16}$$

where $(A_b/\Omega)_{step,\infty}$ and $(A_b/\Omega)_{sine,\infty}$ are given by Eqs. (14) and (15), respectively.

DISCUSSION

Since the amplitude-ratio and the phase-shift of FR depends only on IP and OP characteristic functions for a given forcing function, as seen in Eq. (15), we shall discuss FR behavior by examining their characteristic functions below.

1. Low-frequency and High-frequency Values of Characteristic Functions

Expanding characteristic functions defined by Eq. (12) in power series of ω^* and taking the limit when $\omega^*\to 0$, we can obtain the low frequency limiting values:

$$\lim_{\omega^*\to 0}(f_{1R}/u)=1; \quad \lim_{\omega^*\to 0}(f_{1I}/u)=-1; \quad \lim_{\omega^*\to 0}(f_{22R}/u)=1-x_C^3;$$

$$\lim_{\omega^*\to 0}(f_{22I}/u)=-1+x_C^3; \quad \lim_{\omega^*\to 0}(f_{21R}/u)=K_1x_C^3; \quad \lim_{\omega^*\to 0}(f_{21I}/u)=-K_1x_C^3$$

Substituting these into Eqs. (10) and (11), we can easily obtain the low frequency limiting values of IP and OP characteristic functions, and AR and PS characteristic functions:

$$\lim_{\omega^*\to 0}F_{1R}=K_1x_C^3; \quad \lim_{\omega^*\to 0}F_{1I}=0 \tag{17a}$$

$$\lim_{\omega^*\to 0}F_{2R}=1-x_C^3; \quad \lim_{\omega^*\to 0}F_{2I}=0 \tag{17b}$$

$$\lim_{\omega^*\to 0}F_R=1+(K_1-1)x_C^3; \quad \lim_{\omega^*\to 0}F_I=0 \tag{17c}$$

$$\lim_{\omega^*\to 0}AR=\frac{1}{\omega^*[1+\beta_0(1+(K_1-1)x_C^3)]}; \quad \lim_{\omega^*\to 0}PS=-\frac{\pi}{2} \tag{17d}$$

Limiting values of characteristic functions can also be derived by limits of transfer functions in Laplace domain rather than in frequency domain. By expanding $F_1(s)$ and $F_2(s)$ in power series of s and taking the limits when $s\to 0$, we can obtain:

$$\lim_{s\to 0}F_1(s)=K_1x_C^3 \tag{18a}$$

$$\lim_{s\to 0}F_2(s)=1-x_C^3 \tag{18b}$$

Hence, we have:

$$\lim_{s\to 0}F(s)=\lim_{s\to 0}[F_1(s)+F_2(s)]=1+(K_1-1)x_C^3 \tag{18c}$$

Eq. (17) can be obtained directly from Eq. (18).

Eq. (17) shows that at low frequencies ($\omega^*\to 0$) the adsorption dynamics of the system is much faster than the input modulation, so the equilibrium between the fluid-phase and the particle-phase is established [9]. The distribution between fluid-phase and shell-phase is defined by the term $1/(1-\beta_0x_C^3)$ and the distribution between fluid-phase and core-phase is defined by the term $1/(\beta_0K_1x_C^3)$. We note that the low frequency limiting value of the IP characteristic function depends only on equilibrium parameters of the system.

In the limit when $\omega^*\to 0$, taking the limit of Eq. (15a) and substituting Eq. (17d), we can obtain:

$$\lim_{\omega^*\to 0}\left[\left(\frac{A_b}{\Omega}\right)_{sine,\infty}\right]=\frac{\nu}{1+\beta_0(1+(K_1-1)x_C^3)}\lim_{\omega^*\to 0}\left\{\frac{1}{\omega^*}[1-\cos(\omega^*\tau)]\right\}=0 \tag{19}$$

Thus, taking the limit of Eq. (16) and substituting Eq. (19), we can readily obtain:

$$\lim_{\omega^*\to 0}\frac{A_b}{\Omega}=\left(\frac{A_b}{\Omega}\right)_{step,\infty} \tag{20}$$

where $(A_b/\Omega)_{step,\infty}$ is given by Eq. (14a), which was reported in the reference [21] as mentioned before. Eqs. (19) and (20) mean that the sinusoidal part of FR dissipates and FR becomes the ultimate (i.e., long time) step response in the limit when $\omega^*\to 0$. However, it is not surprising that the ultimate step response is recovered from FR in the limit, since the forcing function given by Eq. (5) becomes unit step function when $\omega^*\to 0$.

For high-frequency limiting values, using the properties of hyperbolic function (e.g., $\tanh(\infty)=\coth(\infty)=1$), we can obtain the following by term-by-term simplification of transfer functions:

$$\lim_{s\to\infty}F_1(s)=0; \quad \lim_{s\to\infty}F_2(s)=0; \quad \lim_{s\to\infty}F(s)=0 \tag{21}$$

Hence, we can obtain the high-frequency limiting values of IP and OP characteristic functions straightforwardly:

$$\lim_{\omega^*\to\infty}F_{1R}=0; \quad \lim_{\omega^*\to\infty}F_{1I}=0 \tag{22a}$$

$$\lim_{\omega^*\to\infty}F_{2R}=0; \quad \lim_{\omega^*\to\infty}F_{2I}=0 \tag{22b}$$

$$\lim_{\omega^*\to\infty}F_R=0; \quad \lim_{\omega^*\to\infty}F_I=0 \tag{22c}$$

$$\lim_{\omega^*\to 0}AR=\frac{1}{\omega^*}; \quad \lim_{\omega^*\to 0}PS=-\frac{\pi}{2} \tag{22d}$$

Eq. (22) shows that at high frequencies ($\omega^*\to\infty$) the input modulations are so fast that no adsorption takes place, and the system behaves as an empty tank without adsorbent [9].

For a more consistent comparison between simulation results, later in the simulation section, we define the reduced characteristic functions based on the low-frequency limiting value of IP characteristic function given by Eq. (17c):

$$\eta_R=\frac{F_R}{1+(K_1-1)x_C^3}; \quad \eta_I=\frac{F_I}{1+(K_1-1)x_C^3}; \tag{23a}$$

$$\eta_{1R}=\frac{F_{1R}}{1+(K_1-1)x_C^3}; \quad \eta_{1I}=\frac{F_{1I}}{1+(K_1-1)x_C^3}; \tag{23b}$$

$$\eta_{2R}=\frac{F_{2R}}{1+(K_1-1)x_C^3}; \quad \eta_{2I}=\frac{F_{2I}}{1+(K_1-1)x_C^3}; \tag{23c}$$

2. Characteristic Function for Inert-core Adsorbent

When $K_1=0$, the inner core of the core-shell composite becomes impermeable. The core-shell adsorbent with impermeable core is called the inert-core adsorbent. FR for the case of the inert-core adsorbent is reported in the reference [20].

Taking the limit when $K_1\to 0$ for characteristic functions defined in Eqs. (9)-(12), we can obtain the following characteristic functions for the inert-core adsorbent through a somewhat tedious simplification procedure:

$$F_R=\frac{n_1d_1+n_2d_2}{d_1^2+d_2^2}; \quad F_I=\frac{n_1d_2-n_2d_1}{d_1^2+d_2^2} \tag{24a}$$

$$n_1=3\Big[\{\cosh[2u(1-x_C)]-\cos[2u(1-x_C)]\} - u(1-x_C)\{\sinh[2u(1-x_C)]+\sin[2u(1-x_C)]\}\Big] \tag{24b}$$

$$n_2=3\Big[-2u^2x_C\{\cosh[2u(1-x_C)]-\cos[2u(1-x_C)]\} - u(1-x_C)\{\sinh[2u(1-x_C)]-\sin[2u(1-x_C)]\}\Big] \tag{24c}$$

$$d_1=-2u^3\left[\frac{1}{\xi}+\left(1-\frac{1}{\xi}\right)x_C\right]\{-\sinh[2u(1-x_C)]+\sin[2u(1-x_C)]\} + \frac{4u^4x_C}{\xi}\{\cosh[2u(1-x_C)]-\cos[2u(1-x_C)]\} \tag{24d}$$

$$d_2=-2u^2\left(1-\frac{1}{\xi}\right)\{\cosh[2u(1-x_C)]-\cos[2u(1-x_C)]\} -2u^3\left[\frac{1}{\xi}+\left(1-\frac{1}{\xi}\right)x_C\right]\{\sinh[2u(1-x_C)]+\sin[2u(1-x_C)]\} \tag{24e}$$

We note that a typographical error in reference [20] is corrected here in Eq. (24d) (the term $\sinh[2u(1-x_C)]$ in Eq. (9d) in the reference is corrected as $(-\sinh[2u(1-x_C)])$). As a result of this correc-

tion, the low frequency limiting values of characteristic functions in the reference [20] have to be replaced by Eq. (17c).

3. Simulation

IP and OP characteristic functions are simulated for the case of $a=1/10^{1.5}$, $\xi=1$, $x_C=0.6$ and $K_1=1$. Usually, for a composite with permeable core, the contact interference at the core-shell interface is negligible; hence K_1 is equal to unity. Whereas for the composite with impermeable core (i.e., inert-core adsorbent) K_1 is equal to zero. The simulated results for $K_1=0$ and $K_1=1$ are shown together in Fig. 1 to show the effect of the permeable core-phase. For $K_1=1$, the OP curve exhibits a bimodal peak and the IP curve exhibits two plateaus. Each pair of peak and plateau is responsible for each phase of the composite. According to Eq. (7b), $F_1(s)$ and $F_2(s)$ are transfer functions relating fluid-phase concentration to core-phase concentration, and relating fluid-phase concentration to shell-phase concentration, respectively. Hence, under the interaction between the core-phase and the shell-phase of the composite, both the response of the core-phase and the response of the shell-phase subject to a periodic modulation of inlet molar flow-rate exhibit their own peaks on the out-of-phase characteristic curve and their own plateaus on the in-phase characteristic curve, respectively. One pair of peak and plateau represents the equilibrium and dynamic characteristics of core-phase, while another pair of peak and plateau represents the equilibrium and dynamic characteristics of shell-phase. To separate the overall characteristic function into the shell and the core characteristic function, which should be required to discriminate between two phases in the composite, the features of the two phases such as peaks or plateaus should have comparable magnitudes with different frequency spectra. The bimodal form of the OP characteristic function and two plateaus of the IP characteristic function constitute unusual characteristics of FR for the core-shell composite which cannot be described by FR for $K_1=0$. Fig. 2 shows FR with the same values of mass transfer parameters as those used in Fig. 1. Other parameters for Fig. 2 are $\beta_0=0.5$, $\nu=1$, $\omega^*=1$.

Fig. 3 shows the effect of the external diffusion parameter on the characteristic function for the case of $K_1=1$, $a=0.1$ and $x_C=0.6$. The intersection between the IP and OP characteristic functions is caused mainly by a surface barrier effect [4]. As can be seen, the crossover frequency between the IP and OP characteristic functions increases with increasing ξ. This is because with increasing ξ the external diffusion resistance increases, so the peak of the OP curve and the plateau of the IP curve for the shell-phase appear in the higher

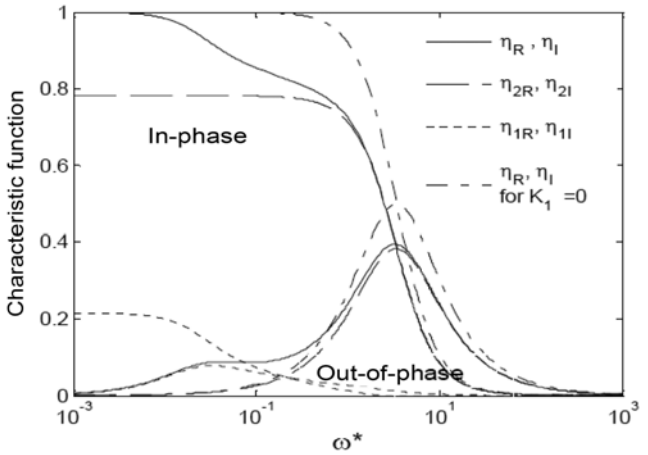

Fig. 1. Typical characteristic function. $K_1=1$, $\xi=1$, $x_C=0.6$, $a=1/10^{1.5}$ and $\xi=1$.

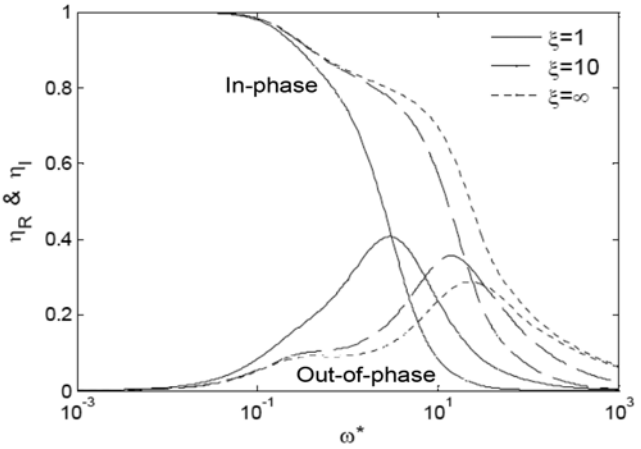

Fig. 3. Effect of external diffusion parameter on characteristic function. $K_1=1$, $x_C=0.6$ and $a=0.1$.

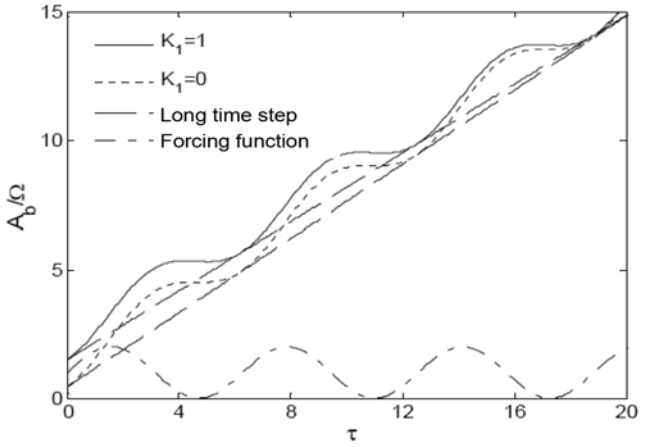

Fig. 2. Typical frequency response. $\xi=1$, $x_C=0.6$, $a=1/10^{1.5}$, $\beta_0=0.5$, $\nu=1$ and $\omega^*=1$.

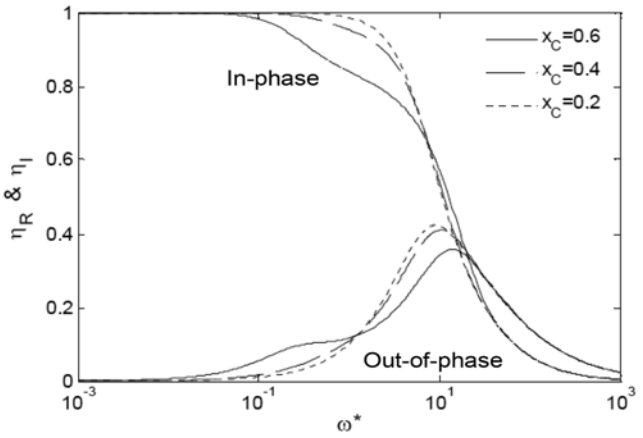

Fig. 4. Effect of core radius on characteristic function. $K_1=1$, $\xi=10$ and $a=0.1$.

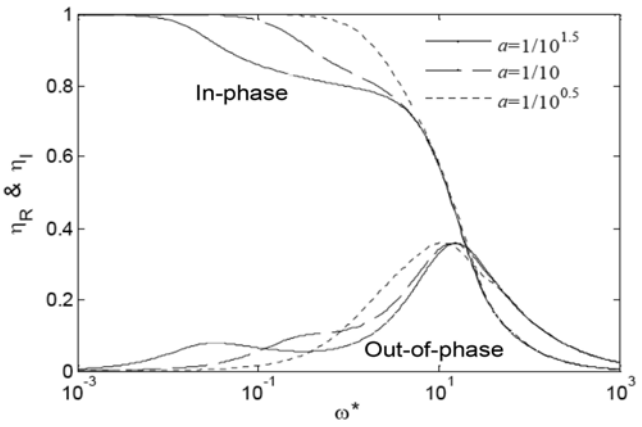

Fig. 5. Effect of core diffusion parameter on characteristic function. K_1=1, ξ=10 and x_C=0.6.

frequency region.

Fig. 4 shows the effect of the core radius x_C on the characteristic function for the case of K_1=1, a=0.1 and ξ=10. With increasing x_C, the first peak of the OP characteristic function and the second plateau of the IP characteristic function appear more clearly. This is because the ratio of the equilibrium capacity of the core-phase to the equilibrium capacity of the shell-phase (i.e., $\beta_0 K_1 x_C^3/(1-\beta_0 x_C^3)$) becomes larger with increasing x_C.

Fig. 5 shows the effect of the core diffusion parameter a on the characteristic function for the case of K_1=1, x_C=0.6 and ξ=10. With decreasing a, the first peak of the OP characteristic function and the second plateau of the IP characteristic function appear more clearly. This is because the diffusion resistance of the core-phase relative to the diffusion resistance of the shell-phase increases with decreasing a. Moreover, the diffusion characteristics of the core-phase appears in the range of lower frequencies with decreasing a. Therefore, experiments should be carried out in the lower frequencies to extract more reliable values of the core diffusion parameter. In the practical measurements of adsorption equilibrium and dynamics, one of the main limitations of the FR technique arises from the limited range of angular frequencies experimentally obtainable. The range of angular frequency covered in the reported literature ranges from 1×10^{-4} rad/s to 60 rad/s, corresponding to the dynamic time-scale range of about 0.015-1×10^5 s [5,22]. For example, if the dynamic time scale is of the order of 10^2 s, the angular frequency is of the order of 10^{-3} rad/s for ω^*=0.1 [since $\omega=\omega^*/(R^2/D_2)=0.1/1\times10^2=1\times10^{-3}$]. In this case we should introduce a sinusoidal forcing function with a period of about 6,000 s. This kind of measurement would be a somewhat time-consuming procedure.

As shown in Eq. (17), the low frequency limiting value of the IP characteristic function of FR depends only on the equilibrium parameters of the system. Hence, in the practical adsorption operation, the low frequency asymptote of the IP characteristic curve can be utilized to extract the equilibrium parameters. Additional information is needed to extract the equilibrium parameters K_1 and K_2 (or β_0). This additional information for the equilibrium parameters could be obtained from the constant term on the RHS of Eq. (15a), which gives a constant shift in FR. For the dynamic parameters, other characteristics of the IP and OP characteristic curves (e.g., peak characteristics of OP characteristic curves, decay characteristics of IP characteristic curve, crossover frequency between the two characteristic curves) over a full frequency spectrum could be utilized.

CONCLUSION

Frequency response behavior of the adsorption vessel containing permeable core-shell composites is theoretically investigated. The low frequency limiting value of in-phase characteristic function depends only on equilibrium parameters of the system. OP characteristic function exhibits bimodal peak and IP characteristic function exhibits two plateaus. Under the interaction between the core-phase and the shell-phase of the composite, both the response of the core-phase and the response of the shell-phase subject to a periodic modulation of inlet molar flow-rate exhibit their own peaks on the out-of-phase characteristic curve and their own plateaus on the in-phase characteristic curve, respectively. One pair of peak and plateau represents the equilibrium and dynamic characteristics of core-phase, while another pair of peak and plateau represents the equilibrium and dynamic characteristics of shell-phase. To separate the overall characteristic function into the shell and the core characteristic function, which should be required to discriminate between two phases in the composite, the features of the two phases such as peaks or plateaus should have comparable magnitudes with different frequency spectra. With increasing in the core radius x_C and decreasing in the core diffusion parameter a, the contribution of the core-phase on the characteristic functions becomes larger, so the first peak of the out-of-phase characteristic curve and the second plateau of the in-phase characteristic curve appear more clearly. With increasing in the external diffusion parameter ξ, the crossover frequency between the in-phase and out-of-phase characteristic curves increases.

ACKNOWLEDGMENT

This work was supported by the Kyungnam University Research Fund, 2009.

NOMENCLATURE

A, A_1, A_2, A_b : dimensionless concentration in composite, core-phase, shell-phase and fluid-phase, respectively, defined in Table 1
AR : amplitude-ratio characteristic function
a : dimensionless core diffusion parameter, defined in Table 1
C : concentration in the particle phase [mol/m^3]
C_0 : reference concentration, on which dimensionless concentration is based [mol/m^3]
C_b : concentration in the fluid phase [mol/m^3]
C_1, C_2: concentration in the core and the shell within particle, respectively [mol/m^3]
D_1, D_2: effective diffusivity in the core and shell, respectively [m^2/s]
F(s) : vessel transfer function
G(s) : overall transfer function relating the forcing function to the response in Laplace domain
K_1, K_2: dimensionless contact affinity at core-shell interface and fluid-particle interface, respectively
k_f : mass transfer coefficient of external diffusion [m/s]
$\dot{N}$: molar flow rate of adsorbate into vessel [mol/sec]
PS : phase-shift characteristic function

R : radius of adsorbent particle [m]
R_C : radius of inert core [m]
r : radius variable of adsorbent particle [m]
t : time variable [s]
V, V_b : volume of total particles including cores and shells and volume of fluid phase within the vessel, respectively [m^3]
x, x_C : dimensionless radius variable of composite and core, defined in Table 1
β_0 : dimensionless distribution parameter, defined in Table 1
δ_R, δ_I : in-phase and out-of-phase characteristic function
η_R, η_I : reduced in-phase and out-of-phase characteristic function based on the low-frequency limiting value of in-phase characteristic function
ξ : dimensionless external diffusion parameter, defined in Table 1
ν : relative amplitude of sinusoidal forcing function, defined in Eq. (5)
τ : dimensionless time variable, defined in Table 1
Ω : dimensionless inlet molar flow-rate, defined in Table 1
ω : angular frequency of sinusoidal forcing function [rad/s]
ω^* : dimensionless angular frequency of sinusoidal forcing function, defined in Table 1

REFERENCES

1. Y. Yasuda and M. Saeki, *J. Phys. Chem*., **82**, 74 (1978).
2. Y. Yasuda, *J. Phys. Chem*., **86**, 1913 (1982).
3. Y. Yasuda, *J. Phys. Chem*., **97**, 3314 (1993).
4. L. M. Sun, G. M. Zhong, P. G. Gray and F. Meunier, *J. Chem. Soc. Faraday Trans*., **90**, 369 (1994).
5. R. G. Jordi and D. D. Do, *Chem. Eng. Sci*., **48**, 1103 (1993).
6. D. Shen and L. V. C. Rees, *J. Chem. Soc. Faraday Trans*., **90**, 3011 (1994).
7. G. Onyestyak and A. Bota, *Micropor. Mesopor. Mater*., **120**, 84 (2009).
8. S. Ngai and V. G. Gomes, *Ind. Eng. Chem. Res*., **35**, 1475 (1996).
9. I.-S. Park, M. Petkovska and D. D. Do, *Chem. Eng. Sci*., **53**, 819 (1998).
10. I.-S. Park, M. Petkovska and D. D. Do, *Chem. Eng. Sci*., **53**, 833 (1998).
11. J. Lee and D. H. Kim, *Chem. Eng. Sci*., **56**, 6711 (2001).
12. B. K. Sward and M. D. LeVan, *Adsorption*, **9**, 37 (2003).
13. M. Chanda and G. L. Rempel, *Ind. Eng. Chem. Res*., **36**, 2190 (1997).
14. X. Ding, Y. Jiang, K. Yu, H. Bala, N. Tao, J. Zhao and Z. Wang, *Mater. Lett*., **58**, 1722 (2004).
15. K. Sakiyama, K. Koga, T. Seto, M. Hirasawa and T. Orii, *J. Phys. Chem. B*, **108**, 523 (2004).
16. D.-G. Yu and J.-H. An, *Colloids Surf. A: Physicochem. Eng. Aspects*, **237**, 87 (2004).
17. W. Fu, H. Yang, L. Chang, M. Li, H. Bala, Q. Yu and G. Zou, *Colloids Surf. A: Physicochem. Eng. Aspects*, **262**, 71 (2005).
18. H. Yang, Z. E. Cao, X. Shen, J. L. Jiang, Z. Q. Wei, J. F. Dai and W. J. Feng, *Mater. Lett*., **63**, 655 (2009).
19. I.-S. Park, *Korean J. Chem. Eng*., **22**, 729 (2005).
20. I.-S. Park, *Korean J. Chem. Eng*., **22**, 960 (2005).
21. I.-S. Park, *Korean J. Chem. Eng*., **23**, 292 (2006).
22. L. Song, Z. Sun, L. Duan, J. Gui and G. S. McDougall, *Micropor. Mesopor. Mater*., **104**, 115 (2007).